Hindawi
Journal of Immunology Research
Volume 2022, Article ID 1825490, 13 pages
https://doi.org/10.1155/2022/1825490

Research Article

miR-181a-5p Inhibits Pyroptosis in Sepsis-Induced Acute Kidney Injury through Downregulation of NEK7

Meng Zhang, Deyuan Zhi, Jin Lin, Pei Liu, Yajun Wang, and Meili Duan

Department of Critical Care Medicine, Beijing Friendship Hospital, Capital Medical University, No. 95 Yong'an Road, Xicheng District, Beijing 100050, China

Correspondence should be addressed to Meili Duan; dmeili@ccmu.edu.cn

Received 12 May 2022; Revised 27 June 2022; Accepted 7 July 2022; Published 10 August 2022

Academic Editor: Lingzhang Meng

Sepsis is a life-threatening organ dysfunction caused by the uncontrolled inflammation, easily affecting the kidney. Sepsis-induced acute kidney injury (S-AKI) has high morbidity and mortality, of which the pathophysiological mechanisms have not been completely illuminated, leading to nonspecific therapies. Specific microRNAs were related with the pathogenesis of AKI. However, only limited studies focused on the pyroptosis in the context of S-AKI. The in vitro LPS-induced HK-2 cell model and in vivo CLP-induced mouse model were established. qRT-PCR, Western blot, ELISA, and RNA pulldown were used for expression examination. Multiple biological databases were used for miRNA screening. H&E staining and IHC staining were performed. The LPS-induced HK-2 cells showed significantly increased ($P < 0.01$) fluorescence intensity of N-GSDMD and ASC compared with the HK-2 cells. The expression of NLRP3, NEK7, ASC, active caspase-1, and N-GSDMD was significantly enhanced ($P < 0.05$) and the inflammatory factors including IL-18, IL-1β, and THF-α were all increased in LPS-induced HK-2 cells and CLP-induced mice. Renal edema, serum Cr and BUN, and expression of KIM-1 and NGAL were significantly higher ($P < 0.05$) in CLP-induced S-AKI mice than the sham group. miR-101-3p, miR-144-3p, miR-181a-5p, miR-4262, and miR-513b-5p could inhibit NEK7. NEK7 is an interacting protein of miRNA-181a-5p. miR-181a-5p inhibits pyroptosis of the LPS-induced HK-2 cells through downregulation of NEK7. Pyroptosis of HK-2 cells promotes inflammation. miR-181a-5p inhibits pyroptosis through downregulation of NEK7 in LPS-induced HK-2 cells and CLP-induced mice. Our study indicated miR-181a-5p as a new potential therapeutic target for S-AKI therapy.

1. Introduction

Sepsis is a life-threatening organ dysfunction caused by the uncontrolled inflammation of the body, of which infection is the common cause [1]. Prevention of organ dysfunction is the key to the treatment of sepsis [2]. The kidney is one of the organs easily affected by sepsis [3]. The incidence of sepsis-induced acute kidney injury (S-AKI) in the intensive care unit is extremely high, and it is one of the risk factors for death in patients with sepsis [4]. S-AKI has high morbidity and mortality especially in young children and old adults, coming with heavy burdens both on the health and economy [5, 6]. As defined by KDIGO (kidney disease: improving global outcomes), S-AKI is characterized by an increase in serum creatinine (Cr) within 48 hours and extremely low urine output and manifested as a clinical syndrome of water electrolyte and acid base balance disorders and azotemia [7].

The mechanisms underlying pathophysiological change of S-AKI have not been completely illuminated, leading to nonspecific therapies [8]. Microcirculatory dysfunction, inflammatory response, and metabolic reprogramming may be associated with S-AKI [9–11]. During sepsis, pathogenic bacteria invade the body and release pathogen-associated molecular patterns (PAMPs), such as lipopolysaccharide (LPS), DNA, and lipoteichoic acid, which combine with the body's pattern recognition receptors (PRR) to initiate the body's immune response and subsequent pro- and anti-inflammatory responses [12]. In addition, after this process

is initiated, certain cells in the body are bound to be damaged or destroyed, which in turn will release cellular contents such as damage-associated molecular patterns (DAMPs). DAMP can also combine with PRR, thereby expanding the body's immune response and inflammatory response.

Different from cell apoptosis, pyroptosis is essentially an innate immune response that can be triggered by the process by which host PRR recognize structures, DAMPs, and conserved PAMPs [13]. There are two pathways found to trigger pyroptosis [14]. One is the canonical inflammasome pathway, that is, the inflammasome pathway mediated by caspase-1, NLRP1, NLRP3, NLRC4, AIM2, and pyrin-inflammasome pathway [15]. The other is noncanonical inflammasome pathway, that is, the inflammasome pathway mediated by caspase-4/5/11 [16]. Pyroptosis is a novel programmed cell death, also known as GSDMD-mediated programmed necrosis, triggered by disturbance of extracellular or intracellular homeostasis associated with innate immunity [17]. Morphologically, pyroptosis is accompanied by features of necrosis and apoptosis. The early stages of pyroptosis produce chromatin condensation and DNA fragmentation, followed by the formation of necrotic-like cell membrane pores, cell swelling, and membrane rupture, leading to the release of cellular contents and proinflammatory mediators, including IL-1β and IL-18 [18].

MicroRNAs regulate gene expression, thus diverse cellular and physiological processes. Extensive studies have indicated a plethora of specific microRNAs in the pathogenesis of AKI [19]. However, only limited studies focused on the pyroptosis in the context of S-AKI. In this study, the miR-181a-5p was screened out. By establishing the LPS-induced HK-2 cell model and CLP-induced mouse model, miR-181a-5p was found to inhibit pyroptosis in S-AKI through NEK7. Our study provides a new potential therapeutic target for S-AKI therapy.

2. Materials and Methods

2.1. Cell Culture and Transfection. The human renal tubular epithelial cell line HK-2 was purchased from the Cell Bank of Chinese Academy of Sciences and cultured in DMEM medium (Invitrogen, CA, USA) containing 10% fetal bovine serum (Invitrogen, CA, USA) at 37°C with 5% CO_2. HK-2 cells were incubated with medium containing 1 μg/ml LPS (Sigma, MO, USA) for 24 h. Then, the cells were seeded in a culture plate (0.6 cm, 1 × 106 per ml) and transfected with different miRNAs (RiboBio, Guangzhou, China) by Lipofectamine 3000 (Invitrogen, CA, USA).

2.2. CCK-8 Assay. The CCK-8 assay was performed as reported [20]. Briefly, HK-2 cells were incubated in 96-well plates for 1–4 days. 10 μl CCK-8 reagent (Dojindo, Kumamoto, Japan) was added. After 30 min, the absorbance value at 450 nm was measured and cell viability was calculated in comparison with control.

2.3. Immunofluorescence Staining. As previously reported, the cultured cells were incubated with fluorescently labeled N-GSDMD and ASC for 30 min [21]. Then, the cells were washed with PBS (pH = 7.4) three times. After adding DAPI (1 μl), the fluorescence localization and intensity were observed by a fluorescence microscope (Nikon, Japan).

2.4. Western Blot. After extracting the total proteins from cells and tissues, the separation was performed by 10% SDS-PAGE [22]. Then, the proteins were transferred to the PVDF membrane, followed by blocking for 1 h. Primary antibodies including anti-caspase-1 (ab62698, 1 : 1000, Abcam), anti-ASC protein (13833, 1 : 1000, Cell Signaling Technology), anti-GSDMD (39754, 1 : 1000, Cell Signaling Technology), anti-NLRP3 (13158, 1 : 1000, Cell Signaling Technology), and GAPDH (ab8245, 1 : 3000, Abcam) and the corresponding secondary antibodies were used. A hypersensitive ECL (BiossciBio, Hubei, China) was used for detection.

2.5. ELISA and Serum Biochemical Examination. The blood was obtained and centrifuged for 10 min. The levels of inflammatory factors in serum including TNF-α, IL-1β, and IL-18 were measured by ELISA kits (Invitrogen, CA, USA). The levels of serum Cr and blood urea nitrogen (BUN) were examined by an automatic biochemical analyzer.

2.6. qRT-PCR. The TRIzol regent (Invitrogen, CA, USA) was used to isolate the total RNA, which was reversely transcribed into cDNA. Subsequently, real-time PCR was conducted using the following primers: NEK7: forward: 5′-GGCAAGATCGCCGTGTAATAATTCTTCAGGTGTTG CTGTTAACATT-3′, reverse: 5′-CTCGAAGCGGCCGGCC GCCCCGACTCAATTTTCAAAGCTAATAACAGA-3′; L-FABP: forward: 5′-GCAGAGCCAGGAGAACTTTG-3′, reverse: 5′-CCTTCCCTTTCTGGATGAGGT-3′; KIM-1: forward: 5′-CTCTAAGCGTGGTTGCCTTC-3′, reverse: 5′-TGTTGTCTTCAGCTCGGGAA-3′; NGAL: forward: 5′-GGCCAGTTCACTCTGGGAAA-3′, reverse: 5′-ACAGCT CCTTGGTTCTTCCA-3′; GAPDH: forward: 5′-AATGTGT CCGTCGTGGATCT -3′, reverse: 5′-AGACAACCTGGTC CTCAGTG-3′.

2.7. Dual-Luciferase Reporter Assay. The dual-luciferase reporter assay system (Promega, WI, USA) was used to detect the luciferase reporter gene [23]. The target fragments of the wild type and mutant type were constructed and integrated into the pGL3 vector. Then, the plasmids were transfected with Lipofectamine 3000 (Invitrogen, CA, USA). After 48 h, the luciferase activity was measured.

2.8. CLP-Induced S-AKI Mouse Model Establishment. Male C57BL/6 mice (~20 g) were purchased from Vital River (Beijing, China). As previously reported, the CLP-induced S-AKI mouse model was established [24]. The animal experiment was approved by the ethics committee of Beijing Friendship Hospital. The mice were randomly divided into two groups ($n = 10$) including the CLP group and sham group. The renal tissue of each mouse was collected 24 h later after operation. The water contents in the renal tissues were measured.

2.9. Hematoxylin-Eosin (HE) Staining. The renal tissues were coated by paraffin, sliced, dewaxed, and hydrated by xylene. The sections were stained with hematoxylin for 5 min and eosin

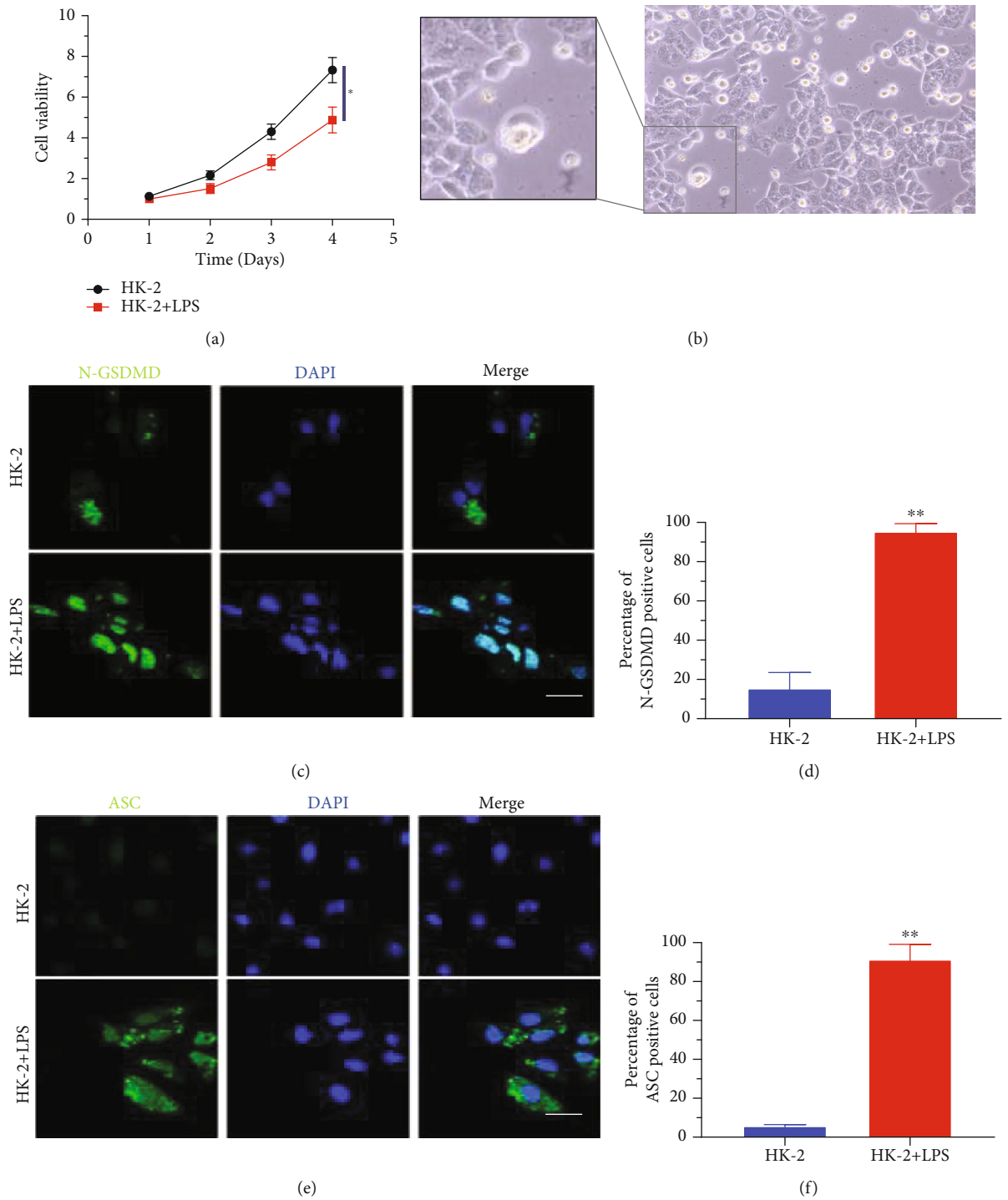

Figure 1: Pyroptosis of the LPS-induced HK-2 cells. (a) Cell viability of HK-2 and LPS-induced HK-2 cells. (b) Morphology of LPS-induced HK-2 cells under optical microscope (200x). (c) Immunofluorescence staining of N-GSDMD and (d) percentage of N-GSDMD-positive cells. (e) Immunofluorescence staining of ASC and (f) percentage of ASC-positive cells. $^{**}P < 0.01$.

for 30 s, followed by scoring of tubular damage into 0 (none), 1 (1–10%), 2 (11–25%), 3 (26–45%), and 4 (46–75%) [25].

2.10. IHC Staining. The immunohistochemistry (IHC) staining of the renal tissues was performed to examine the expression of caspase-1, N-GSDMD, NEK7, and NLPR3 [26].

2.11. TUNEL Staining. The terminal deoxynucleotidyl transferase-mediated dUTP nick end labeling (TUNEL) staining was performed to examine the cell apoptosis [27].

2.12. RNA Pulldown. The RNA overexpression plasmids were constructed and verified [28]. Then, the primers

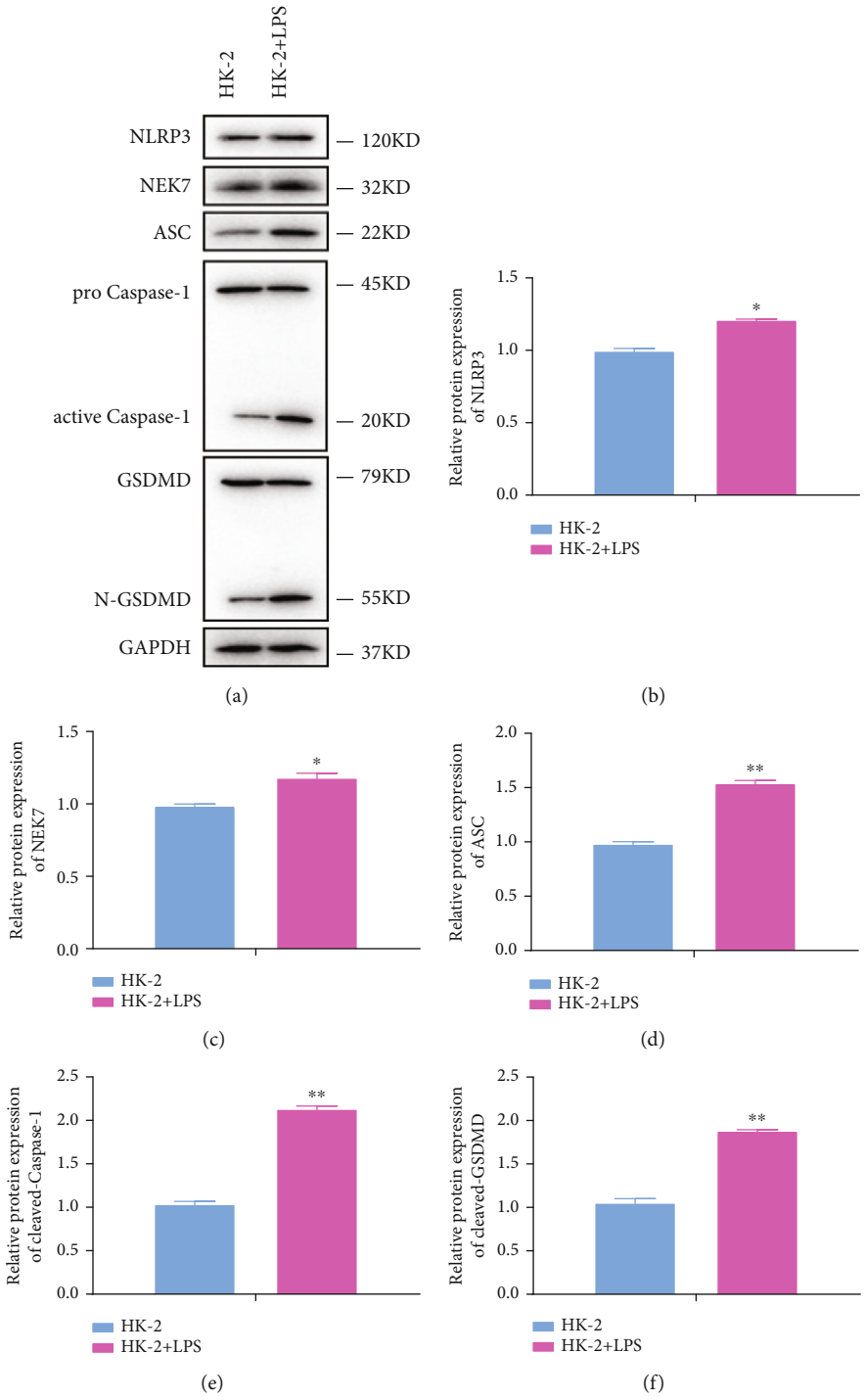

Figure 2: Continued.

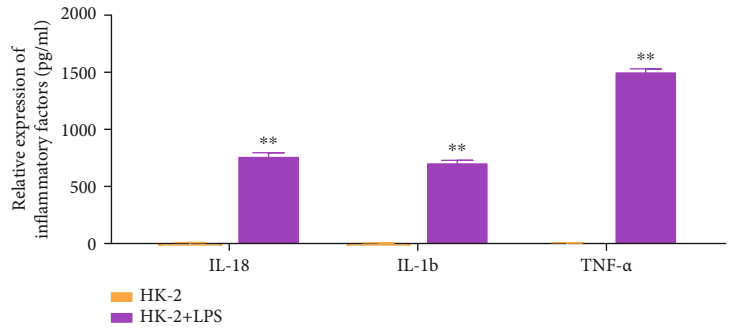

(g)

Figure 2: Pyroptosis of HK-2 cells promotes inflammation. (a) The protein expression of NLRP3, NEK7, ASC, active caspase-1, and N-GSDMD in HK-2 and LPS-induced HK-2 cells by Western blot, and (b–f) quantification by ImageJ. (g) The expression of inflammatory factors including IL-18, IL-1β, and THF-α by ELISA. $^{*}P < 0.05$, $^{**}P < 0.01$.

containing the T7 promoter were designed and amplified to obtain the transcription template. The PCR product was used as template to obtain the target RNA. The interacting proteins were enriched by magnetic bead-RNA probe complexes, followed by SDS-PAGE electrophoresis silver staining to detect the enriched proteins.

2.13. Statistical Analysis. Multiple databases including TargetScan database, miRDB database, miCode database, and DIANA-TarBase database were used to screen miRNAs regulating NEK7 gene expression. GraphPad Prism 8.0 (IBM, USA) was used for data analysis. Data are presented as mean ± standard deviation. The t-test and analysis of variance (ANOVA) were conducted to analyze the differences. $P < 0.05$ was statistically significant.

3. Results

3.1. Pyroptosis of the LPS-Induced HK-2 Cells. In the LPS-induced HK-2 cells, the cell viability was reduced (Figure 1(a)) and apical vacuolization was observed, indicating pyroptosis (Figure 1(b)). The fluorescent staining of N-GSDMD and ASC was performed to locate pyroptotic cells and evaluate the degree of pyroptosis. As shown in Figures 1(c) and 1(d), the LPS-induced HK-2 cells showed significantly increased ($P < 0.01$) fluorescence intensity of N-GSDMD compared with the HK-2 cells. Besides, the fluorescence intensity of ASC was significantly higher ($P < 0.01$) in LPS-induced HK-2 cells than HK-2 cells (Figures 1(e) and 1(f)). The results suggested that obvious pyroptosis was induced by LPS in HK-2 cells.

3.2. Pyroptosis of HK-2 Cells Promotes Inflammation. To study the effect of pyroptosis on inflammation, the expression of several important markers and inflammatory factors was examined. As shown in Figures 2(a)–2(f), the expression of NLRP3, NEK7, ASC, active caspase-1, and N-GSDMD was significantly enhanced ($P < 0.05$) in LPS-induced HK-2 cells by Western blot. Moreover, the inflammatory factors including IL-18, IL-1β, and THF-α were all increased in LPS-induced HK-2 cells by ELISA (Figure 2(g)). As is known, canonical inflammasomes are associated with NLRP3, ASC, and caspase-1, while noncanonical inflammasomes is associated with GSDMD. The results indicated that pyroptosis of HK-2 cells could activate both canonical and noncanonical inflammasomes.

3.3. Renal Injury in the CLP-Induced S-AKI Mouse Model. As shown in Figure 3(a) and S1, the CLP-induced S-AKI mouse model was established. The water content in CLP-induced mice was significantly higher ($P < 0.05$) than that in the sham group (Figure 3(b)), indicating increased renal edema in a CLP-induced S-AKI mouse. To further assess the extent of renal injury, the H&E staining was conducted. As shown in Figures 3(c) and 3(d), increased inflammatory cell infiltration in the renal tissues and a higher pathological damage index (2.72 ± 0.31 vs. 0.20 ± 0.04) were observed in CLP-induced mice. Furthermore, the renal injury-related indicators were measured. As shown in Figure 3(e), the Cr and BUN were significantly higher ($P < 0.05$) in CLP-induced mice than sham group. As shown in Figure 3(f), the mRNA expression of KIM-1 and NGAL was significantly increased ($P < 0.01$) in CLP-induced mice, while L-FABP remained unchanged.

3.4. Pyroptosis of Renal Tubular Epithelial Cells in the CLP-Induced S-AKI Mouse Model. As shown in Figure 4(a), the expression of caspase-1, N-GSDMD, NEK7, and NLRP3 was significantly higher ($P < 0.05$) in CLP-induced mice than the sham group by IHC. Moreover, the protein expression was examined by Western blot as well. As shown in Figures 4(b) and 4(c), the expression of NEK7, NLRP3, ASC, active caspase-1, and N-GSDMD was significantly increased ($P < 0.05$) in CLP-induced mice. Furthermore, the inflammatory factors including IL-1β, IL-18, and THF-α were all increased in CLP-induced mice by ELISA (Figure 4(d)). These results indicated the pyroptosis of renal tubular epithelial cells in the CLP-induced S-AKI mouse model.

3.5. miR-181a-5p Inhibits NEK7 in HK-2 Cells. The miRNAs that regulate NEK7 gene expression were screened through multiple biological information databases. According to the prediction results of TargetScan database, miRDB database, miCode database, and DIANA-TarBase database, the

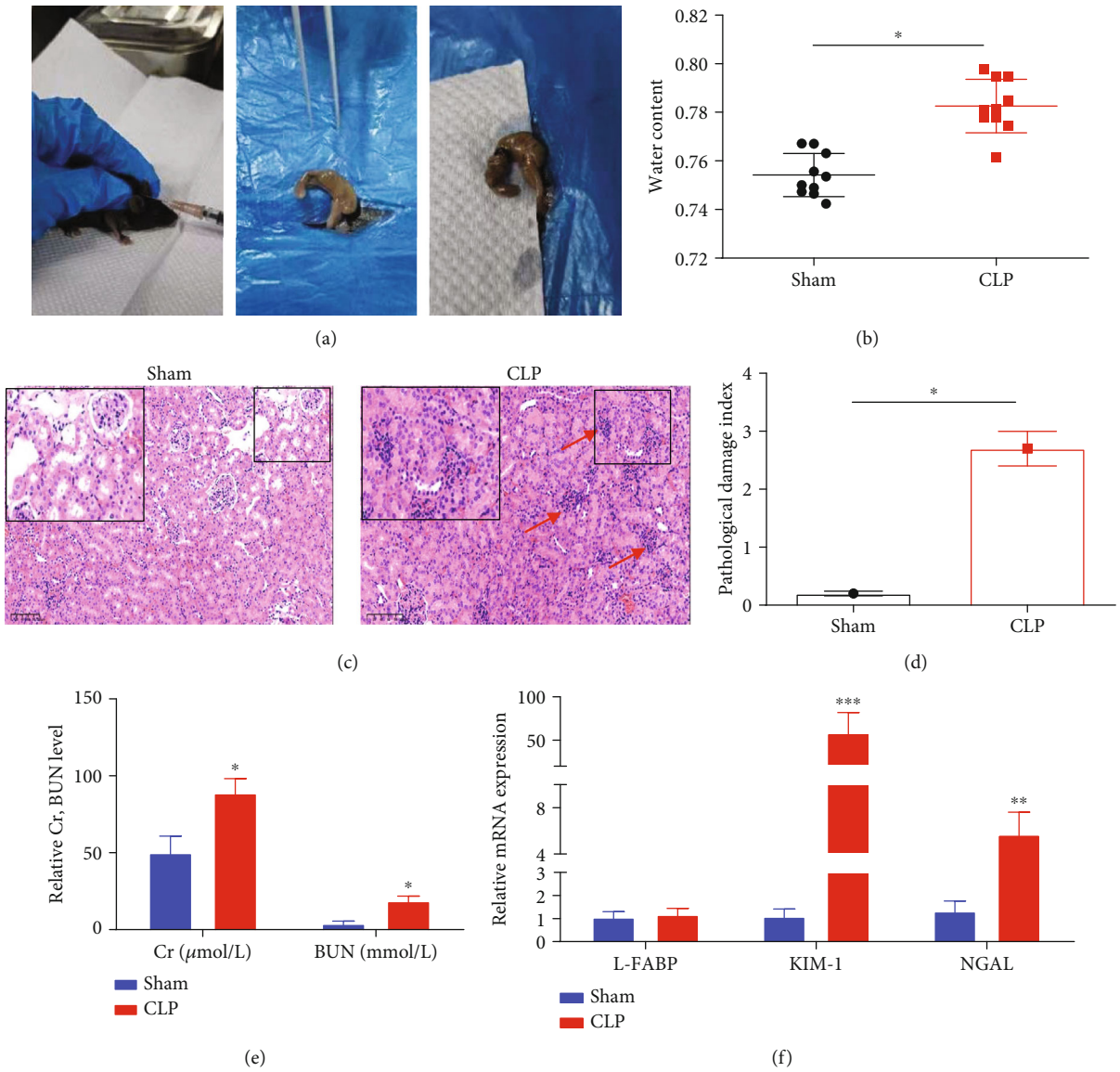

Figure 3: Renal injury in the CLP-induced S-AKI mouse model. (a) The CLP-induced S-AKI mouse model was established. (b) The renal water content in sham and CLP-induced mice. (c) H&E staining of renal tissues. The arrow indicates increased inflammatory cell infiltration. Scale bar = 100 μm. (d) Pathological score. (e) The level of renal injury-related indicators including the serum Cr and BUN. (f) The mRNA expression of L-FABP, KIM-1, and NGAL by qRT-PCR. $^{*}P < 0.05$, $^{**}P < 0.01$, and $^{***}P < 0.001$.

miRNAs supported by more than two databases that have the ability to regulate NEK7 were miR-101-3p, miR-144-3p, miR-181a-5p, miR-4262, miR-582-3p, and miR-513b-5p (Figure 5(a)). Based on the prediction of the abovementioned database, the luciferase reporter gene detection was conducted. As shown in Figure 5(b), five miRNAs including miR-101-3p, miR-144-3p, miR-181a-5p, miR-4262, and miR-513b-5p could inhibit NEK7. The expression of NEK7 in the mRNA level (Figure 5(c)) and protein level (Figure S2, Figures 5(d) and 5(e)) further confirmed this. Of note, the miR-181a-5p exhibited the strongest inhibitory effect. In order to further verify the interaction between miRNA-101-3p, miRNA-181a-5p, miRNA-4262, and NEK7, RNA pulldown experiment was performed after miRNA was transcribed and purified in vitro and the binding protein of miRNA was detected. The results showed that miRNA-181a-5p could interact with NEK7 and it is verified that NEK7 is an interacting protein of miRNA-181a-5p (Figures 5(f) and 5(g)).

3.6. miR-181a-5p Inhibits Pyroptosis of the LPS-Induced HK-2 Cells through Downregulation of NEK7. As shown in Figure 6(a), overexpressed NEK7 promoted and miRNA-181a-5p inhibited pyroptosis of the LPS-induced HK-2 cells. Importantly, the miRNA-181a-5p could partially reverse the increased pyroptosis. Moreover, the results of cell apoptosis by TUNEL were similar (Figures 6(b) and 6(c)), indicating that miRNA-181a-5p could inhibit cell

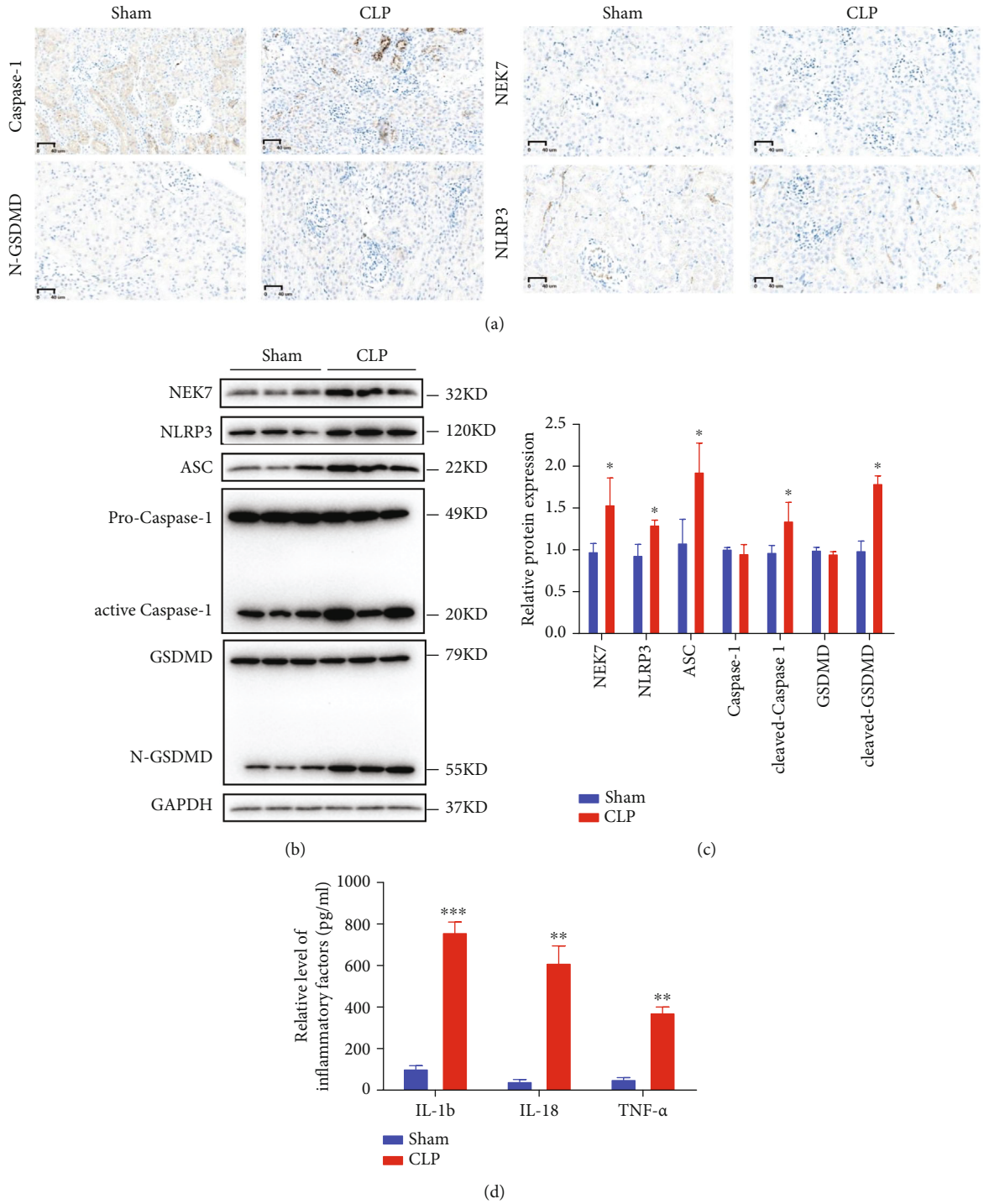

Figure 4: Pyroptosis of renal tubular epithelial cells in the CLP-induced S-AKI mouse model. (a) The expression of caspase-1, N-GSDMD, NEK7, and NLRP3 in sham and CLP-induced mice by IHC. (b) The protein expression of NEK7, NLRP3, ASC, active caspase-1, and N-GSDMD by Western blot, and (c) quantification by ImageJ. (d) The expression of inflammatory factors including IL-18, IL-1β, and THF-α. $^{*}P < 0.05$, $^{**}P < 0.01$, and $^{***}P < 0.001$.

apoptosis through NEK7 as well. Consistently, higher cell viability in NEK7-OE + miRNA-181a-5p mimic than NEK7-OE + NC mimic was observed in Figure 6(d). The miRNA-181a-5p could inhibit expression of NEK7, NLRP3, N-GSDMD, and active caspase-1 and partially reverse the increased expression of these proteins induced by NEK7 (Figures 6(e) and 6(f)). The results in the mRNA level were consistent (Figure S3). The level of inflammatory factors including IL-1β and IL-18 also confirmed this result (Figure 6(g)).

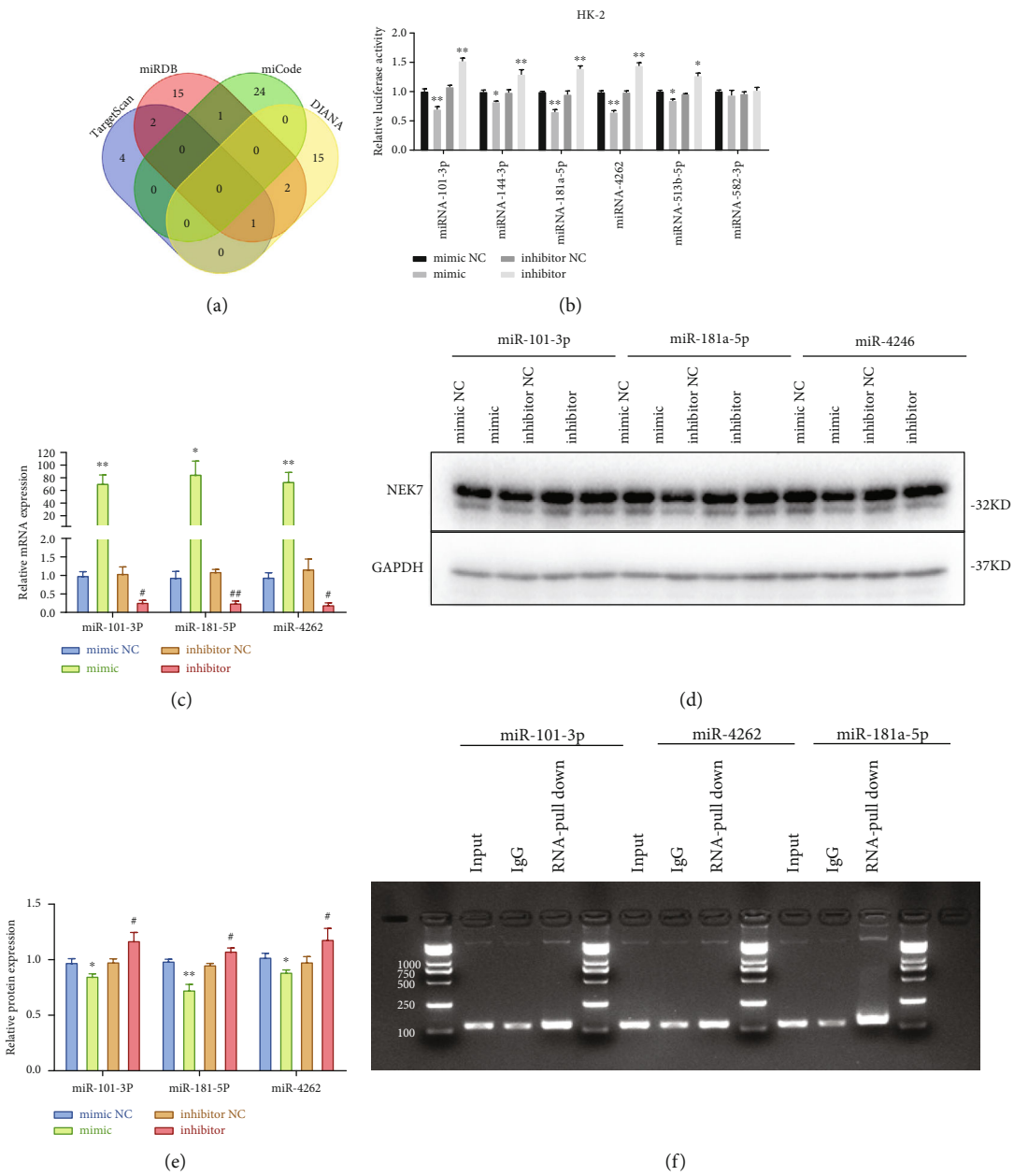

FIGURE 5: Continued.

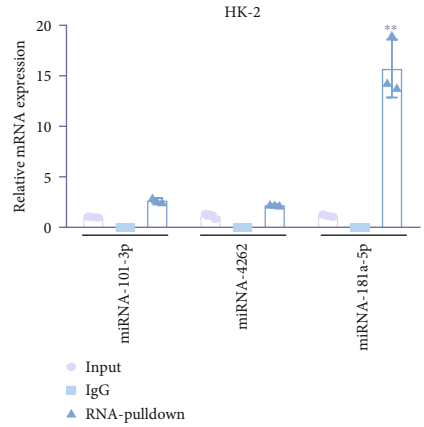

(g)

Figure 5: miR-181a-5p inhibits NEK7 in HK-2 cells. (a) Multiple biological databases including TargetScan database, miRDB database, miCode database, and DIANA-TarBase database to screen the miRNAs that regulate NEK7 gene expression. (b) The luciferase reporter gene detection of eight screened miRNAs. (c) The mRNA expression of NEK7 in the three top significant miRNAs by qRT-PCR. (d) The protein expression of NEK7 in the three top significant miRNAs by Western blot, and (e) quantification by ImageJ. $^{*}P < 0.05$, $^{**}P < 0.01$ compared with mimic NC; $^{\#}P < 0.05$, $^{\#\#}P < 0.01$ compared with inhibitor NC. (f) RNA pulldown of three top significant miRNAs by SDS-PAGE, and (g) quantification by ImageJ. $^{**}P < 0.01$ compared with input or IgG.

4. Discussion

Accumulated evidences have suggested the microRNAs as critical regulators of renal pathophysiology and play important roles in kidney diseases such as S-AKI [29]. Juan et al. reported the exosome-mediated pyroptosis of miR-93-TXNIP-NLRP3 in S-AKI [30]. Deng et al. found that lncRNA PVT1 could modulate NLRP3-mediated pyroptosis targeting miR-20a-5p in S-AKI [31]. MicroRNA-92a-3p was identified as an essential regulator of pyroptosis in renal ischemia-reperfusion injury [32]. The miR-223-3p/NLRP3 pathway is involved in the LPS-induced AKI and inhibits HK-2 cell pyroptosis [33]. The release of microRNA-135b-5p could restrain LPS-induced pyroptotic cell death and inflammation in HK-2 cells [34]. Our study added that miR-181a-5p could inhibit pyroptosis in LPS-induced HK-2 cells and CLP-induced S-AKI mouse model through downregulation of NEK7. Yan and Huang found that miR-181a-5p overexpression could reversed the inhibitory effect of total glucosides of paeony on the pyroptosis of hypoxia/reoxygenation cardiomyocytes, indicating the relation between miR-181a-5p and pyroptosis by cell experiments [35]. Wang et al. reported that increased miR-181a-5p could aggravate kidney injury in sepsis via the PPARα pathway by cell experiments [23]. This study is the first time to report the association of miR-181a-5p and pyroptosis in S-AKI by establishing the in vitro LPS-induced HK-2 cell model and in vivo CLP-induced S-AKI mouse model.

The association of S-AKI and pyroptosis remains to be better understood. There are only two studies reporting this. Zhang et al. found that downregulated IRF2 could alleviate S-AKI in vitro and in vivo [36]. Liu and Wang found that the DRP1 inhibitor could alleviate LPS-reduced S-AKI by inhibiting NLRP3 inflammasome [37]. Pyroptosis has long been considered to be caspase-1-mediated death of monocytes following infection by certain bacteria [38]. Caspase-1 is activated by different inflammasomes during various infections and immune responses. The inflammasome is a multiprotein complex with an inherent ability to induce an innate immune response by sensing damage signals and microbial attack and is present in the cytoplasm of many types of cells, including immune cells, neural cells, microglia, astrocytes, and lung endothelial cells [39]. The basic structure of most inflammasomes is composed of the nucleotide-binding oligomerization domain-like receptor (NLR) family and AIM2-like receptor (ALR) protein family as receptor proteins, apoptosis-associated speck-like protein (ASC) as adaptor protein, and caspases as effector protein [40]. Recent research has reported that GSDMD could form pores on the cell membrane, thereby increasing cell permeability and forming osmotic pressure difference inside and outside cells, which leads to cell swelling and outflow of intracellular substances, finally triggering pyroptosis [41, 42]. Our results also showed that miRNA-181a-5p could inhibit expression of NLRP3, N-GSDMD, and active caspase-1 and partially reverse the increased expression of these proteins induced by NEK7.

The NLRP3 inflammasome is important in immunity and human diseases, which can be activated by diverse stimuli [43]. NEK7 has been reported to be interacted with NLRP3 to modulate the pyroptosis in inflammatory bowel disease via NF-κB signaling [44]. NLRP3-NEK7-complex formation is involved in the initiation of inflammasome assembly and pyroptosis in human macrophages [45]. The inflammasome is activated through two pathways. The first pathway is the activation of the inflammasome when the body is exposed to various endogenous and exogenous stimuli. The recruited caspase-1 is activated in the cell, cleaves IL-1β precursor and IL-18 precursor in the inner side of the plasma membrane, produces mature molecules of IL-1β and IL-18, and releases them to the outside of the cell,

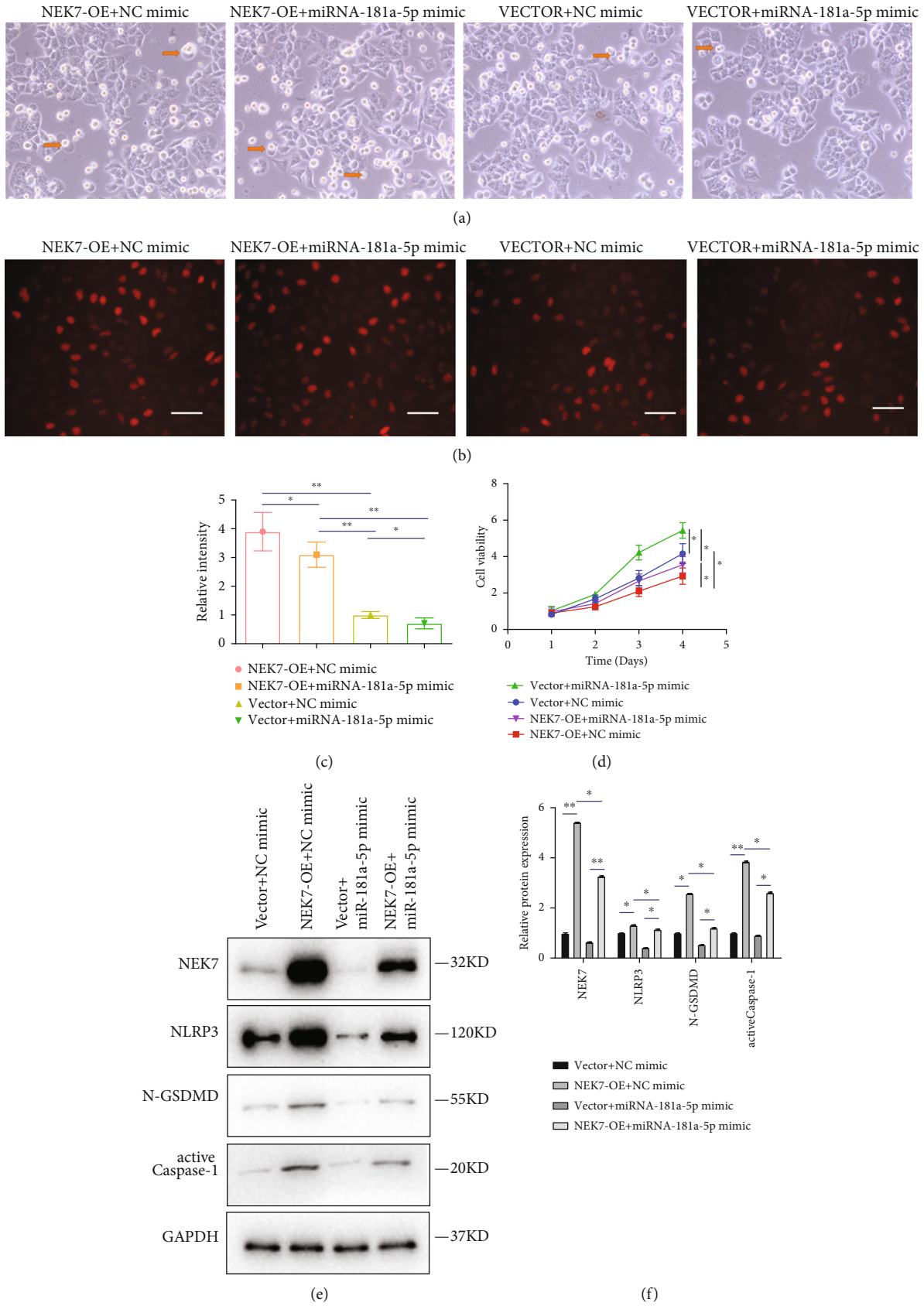

Figure 6: Continued.

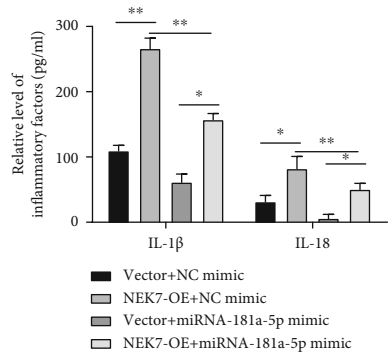

(g)

Figure 6: miR-181a-5p inhibits pyroptosis of the LPS-induced HK-2 cells through downregulation of NEK7. (a) Morphology of LPS-induced HK-2 cells transfected with four vectors under an optical microscope (200x). The red arrow indicates pyroptosis of the cell. (b) Cell apoptosis of LPS-induced HK-2 cells transfected with four vectors by TUNEL, and (c) relative intensity of fluorescence. Scale bar = 100 μm. (d) Cell viability of LPS-induced HK-2 cells transfected with four vectors by CCK-8 assay. (e) The protein expression of NEK7, NLRP3, N-GSDMD, and active caspase-1 by Western blot, and (f) quantification by ImageJ. (g) The expression of inflammatory factors including IL-1β and IL-18. $^{*}P < 0.05$, $^{**}P < 0.01$.

promoting inflammatory response and directly and rapidly activating innate immunity [46]. The second pathway is that when the body is stimulated by stimuli such as LPS, the NF-κB pathway is activated, followed by nuclear translocation of NF-κB to mediate activation of IL-1β and IL-18 precursors to produce IL-1β and IL-18 inflammatory factors for mediating inflammatory and immune responses [47, 48]. Since only the in vitro studies were performed, bioinformatic analysis using open-access database with sepsis population would expand the potential value of its clinical translation. Besides, gene-knockout mice can further validate the current finding. In the future study, we will continue to evaluate the outcomes of inhibiting the target molecule and clarify whether this can ameliorate the severity of AKI.

5. Conclusions

In conclusion, this study revealed the role of miR-181a-5p in pyroptosis of S-AKI. Pyroptosis of HK-2 cells promotes inflammation. miR-181a-5p inhibits pyroptosis through downregulation of NEK7 in LPS-induced HK-2 cells and CLP-induced mice. Our study indicated miR-181a-5p as a new potential therapeutic target for S-AKI therapy.

Data Availability

The original data was available in a necessary request.

Conflicts of Interest

The authors declare that there is no conflict of interest regarding the publication of this paper.

Acknowledgments

The authors thank the Beijing Hospitals Authority Innovation Studio of Young Staff Funding Support, code: 202102, for the support.

Supplementary Materials

See Figure S1 for the procedure of CLP-induced S-AKI mouse model establishment. See Figure S2 for the expression of NEK7 in the protein level. See Figure S3 for the mRNA expression of NEK7, NLRP3, N-GSDMD, and active caspase-1. *(Supplementary Materials)*

References

[1] M. Cecconi, L. Evans, M. Levy, and A. Rhodes, "Sepsis and septic shock," *Lancet (London, England)*, vol. 392, no. 10141, pp. 75–87, 2018.

[2] V. P. Ho, H. Kaafarani, R. Rattan, N. Namias, H. Evans, and T. L. Zakrison, "Sepsis 2019: what surgeons need to know," *Surgical Infections*, vol. 21, no. 3, pp. 195–204, 2020.

[3] R. Bellomo, J. A. Kellum, C. Ronco et al., "Acute kidney injury in sepsis," *Intensive Care Medicine*, vol. 43, no. 6, pp. 816–828, 2017.

[4] J. T. Poston and J. L. Koyner, "Sepsis associated acute kidney injury," *BMJ*, vol. 364, 2019.

[5] R. S. Hotchkiss and I. E. Karl, "The pathophysiology and treatment of sepsis," *The New England Journal of Medicine*, vol. 348, no. 2, pp. 138–150, 2003.

[6] A. Vijayan, "Tackling AKI: prevention, timing of dialysis and follow-up," *Nature Reviews Nephrology*, vol. 17, no. 2, pp. 87-88, 2021.

[7] S. Peerapornratana, C. L. Manrique-Caballero, H. Gómez, and J. A. Kellum, "Acute kidney injury from sepsis: current concepts, epidemiology, pathophysiology, prevention and treatment," *Kidney International*, vol. 96, no. 5, pp. 1083–1099, 2019.

[8] C. L. Manrique-Caballero, G. Del Rio-Pertuz, and H. Gomez, "Sepsis-associated acute kidney injury," *Critical Care Clinics*, vol. 37, no. 2, pp. 279–301, 2021.

[9] E. H. Post, J. A. Kellum, R. Bellomo, and J. L. Vincent, "Renal perfusion in sepsis: from macro- to microcirculation," *Kidney International*, vol. 91, no. 1, pp. 45–60, 2017.

[10] H. R. Jang and H. Rabb, "Immune cells in experimental acute kidney injury," *Nature Reviews Nephrology*, vol. 11, no. 2, pp. 88–101, 2015.

[11] H. Gómez, J. A. Kellum, and C. Ronco, "Metabolic reprogramming and tolerance during sepsis-induced AKI," *Nature Reviews Nephrology*, vol. 13, no. 3, pp. 143–151, 2017.

[12] Y. L. Gao and J. H. Zhai, "Recent advances in the molecular mechanisms underlying pyroptosis in sepsis," *Mediators of Inflammation*, vol. 2018, Article ID 5823823, 7 pages, 2018.

[13] B. E. Burdette, A. N. Esparza, H. Zhu, and S. Wang, "Gasdermin D in pyroptosis," *Acta Pharmaceutica Sinica B*, vol. 11, no. 9, pp. 2768–2782, 2021.

[14] P. Yu, X. Zhang, N. Liu, L. Tang, C. Peng, and X. Chen, "Pyroptosis: mechanisms and diseases," *Signal Transduction and Targeted Therapy*, vol. 6, no. 1, p. 128, 2021.

[15] J. Hou, J. M. Hsu, and M. C. Hung, "Molecular mechanisms and functions of pyroptosis in inflammation and antitumor immunity," *Molecular Cell*, vol. 81, no. 22, pp. 4579–4590, 2021.

[16] Y. Wang, W. Gao, X. Shi et al., "Chemotherapy drugs induce pyroptosis through caspase-3 cleavage of a gasdermin," *Nature*, vol. 547, no. 7661, pp. 99–103, 2017.

[17] J. Shi, W. Gao, and F. Shao, "Pyroptosis: gasdermin-mediated programmed necrotic cell death," *Trends in Biochemical Sciences*, vol. 42, no. 4, pp. 245–254, 2017.

[18] Y. Fang, S. Tian, Y. Pan et al., "Pyroptosis: a new frontier in cancer," *Biomedicine & Pharmacotherapy*, vol. 121, article 109595, 2020.

[19] C. Guo, G. Dong, X. Liang, and Z. Dong, "Epigenetic regulation in AKI and kidney repair: mechanisms and therapeutic implications," *Nature Reviews Nephrology*, vol. 15, no. 4, pp. 220–239, 2019.

[20] H. Cai, R. Wang, X. Guo et al., "Combining gemcitabine-loaded macrophage-like nanoparticles and erlotinib for pancreatic cancer therapy," *Molecular Pharmaceutics*, vol. 18, no. 7, pp. 2495–2506, 2021.

[21] H. Huang, H. Ni, K. Ma, and J. Zou, "ANGPTL2 regulates autophagy through the MEK/ERK/Nrf-1 pathway and affects the progression of renal fibrosis in diabetic nephropathy," *American Journal of Translational Research*, vol. 11, no. 9, pp. 5472–5486, 2019.

[22] H. Cai, X. Dai, X. Guo et al., "Ataxia telangiectasia mutated inhibitor-loaded copper sulfide nanoparticles for low-temperature photothermal therapy of hepatocellular carcinoma," *Acta Biomaterialia*, vol. 127, pp. 276–286, 2021.

[23] J. Wang, J. Song, Y. Li, J. Shao, Z. Xie, and K. Sun, "Down-regulation of LncRNA CRNDE aggravates kidney injury via increasing MiR-181a-5p in sepsis," *International Immunopharmacology*, vol. 79, article 105933, 2020.

[24] R. L. Wilson, V. Selvaraju, R. Lakshmanan et al., "Thioredoxin-1 attenuates sepsis-induced cardiomyopathy after cecal ligation and puncture in mice," *The Journal of Surgical Research*, vol. 220, pp. 68–78, 2017.

[25] Y. Wu, L. Wang, L. Meng, G. K. Cao, Y. L. Zhao, and Y. Zhang, "Biological effects of autophagy in mice with sepsis-induced acute kidney injury," *Experimental and Therapeutic Medicine*, vol. 17, no. 1, pp. 316–322, 2019.

[26] M. N. Kim, J. H. Moon, and Y. M. Cho, "Sodium-glucose cotransporter-2 inhibition reduces cellular senescence in the diabetic kidney by promoting ketone body-induced NRF2 activation," *Diabetes, Obesity & Metabolism*, vol. 23, no. 11, pp. 2561–2571, 2021.

[27] L. Su, X. Jiang, C. Yang et al., "Pannexin 1 mediates ferroptosis that contributes to renal ischemia/reperfusion injury," *The Journal of Biological Chemistry*, vol. 294, no. 50, pp. 19395–19404, 2019.

[28] X. Li, T. K. Ma, S. Wen et al., "LncRNA ARAP1-AS2 promotes high glucose-induced human proximal tubular cell injury via persistent transactivation of the EGFR by interacting with ARAP1," *Journal of Cellular and Molecular Medicine*, vol. 24, no. 22, pp. 12994–13009, 2020.

[29] Z. Liu, S. Wang, Q. S. Mi, and Z. Dong, "MicroRNAs in pathogenesis of acute kidney injury," *Nephron*, vol. 134, no. 3, pp. 149–153, 2016.

[30] C. X. Juan, Y. Mao, Q. Cao et al., "Exosome-mediated pyroptosis of miR-93-TXNIP-NLRP3 leads to functional difference between M1 and M2 macrophages in sepsis-induced acute kidney injury," *Journal of Cellular and Molecular Medicine*, vol. 25, no. 10, pp. 4786–4799, 2021.

[31] L. T. Deng, Q. L. Wang, C. Yu, and M. Gao, "lncRNA PVT1 modulates NLRP3-mediated pyroptosis in septic acute kidney injury by targeting miR-20a-5p," *Molecular Medicine Reports*, vol. 23, no. 4, 2021.

[32] R. Wang, H. Zhao, Y. Zhang et al., "Identification of microRNA-92a-3p as an essential regulator of tubular epithelial cell pyroptosis by targeting Nrf1 via HO-1," *Frontiers in Genetics*, vol. 11, article 616947, 2021.

[33] J. Tan, J. Fan, J. He, L. Zhao, and H. Tang, "Knockdown of LncRNA DLX6-AS1 inhibits HK-2 cell pyroptosis via regulating miR-223-3p/NLRP3 pathway in lipopolysaccharide-induced acute kidney injury," *Journal of Bioenergetics and Biomembranes*, vol. 52, no. 5, pp. 367–376, 2020.

[34] J. Huang and C. Xu, "LncRNA MALAT1-deficiency restrains lipopolysaccharide (LPS)-induced pyroptotic cell death and inflammation in HK-2 cells by releasing microRNA-135b-5p," *Renal Failure*, vol. 43, no. 1, pp. 1288–1297, 2021.

[35] X. Yan and Y. Huang, "Mechanism of total glucosides of paeony in hypoxia/reoxygenation-induced cardiomyocyte pyroptosis," *Journal of Bioenergetics and Biomembranes*, vol. 53, no. 6, pp. 643–653, 2021.

[36] Y. Zhang, Y. Zhang, A. Yang, and F. Xia, "Downregulation of IRF2 alleviates sepsis-related acute kidney injury in vitro and in vivo," *Drug Design, Development and Therapy*, vol. 15, pp. 5123–5132, 2021.

[37] R. Liu and S. C. Wang, "An inhibitor of DRP1 (Mdivi-1) alleviates LPS-induced septic AKI by inhibiting NLRP3 inflammasome activation," *BioMed Research International*, vol. 2020, Article ID 2398420, 11 pages, 2020.

[38] F. Awad, E. Assrawi, C. Louvrier et al., "Inflammasome biology, molecular pathology and therapeutic implications," *Pharmacology & Therapeutics*, vol. 187, pp. 133–149, 2018.

[39] D. A. Muruve, V. Pétrilli, A. K. Zaiss et al., "The inflammasome recognizes cytosolic microbial and host DNA and triggers an innate immune response," *Nature*, vol. 452, no. 7183, pp. 103–107, 2008.

[40] L. Q. Wang, T. Liu, S. Yang et al., "Perfluoroalkyl substance pollutants activate the innate immune system through the AIM2 inflammasome," *Nature Communications*, vol. 12, no. 1, p. 2915, 2021.

[41] K. Wang, Q. I. Sun, X. Zhong et al., "Structural mechanism for GSDMD targeting by autoprocessed caspases in pyroptosis," *Cell*, vol. 180, pp. 941–955.e20, 2020.

[42] J. Shi, Y. Zhao, K. Wang et al., "Cleavage of GSDMD by inflammatory caspases determines pyroptotic cell death," *Nature*, vol. 526, no. 7575, pp. 660–665, 2015.

[43] Y. He, H. Hara, and G. Núñez, "Mechanism and regulation of NLRP3 inflammasome activation," *Trends in Biochemical Sciences*, vol. 41, no. 12, pp. 1012–1021, 2016.

[44] X. Chen, G. Liu, Y. Yuan, G. Wu, S. Wang, and L. Yuan, "NEK7 interacts with NLRP3 to modulate the pyroptosis in inflammatory bowel disease via NF-κB signaling," *Cell Death & Disease*, vol. 10, no. 12, p. 906, 2019.

[45] I. Boal-Carvalho, B. Mazel-Sanchez, F. Silva et al., "Influenza A viruses limit NLRP3-NEK7-complex formation and pyroptosis in human macrophages," *EMBO Reports*, vol. 21, no. 12, article e50421, 2020.

[46] A. Malik and T. D. Kanneganti, "Inflammasome activation and assembly at a glance," *Journal of Cell Science*, vol. 130, no. 23, pp. 3955–3963, 2017.

[47] W. T. He, H. Wan, L. Hu et al., "Gasdermin D is an executor of pyroptosis and required for interleukin-1β secretion," *Cell Research*, vol. 25, no. 12, pp. 1285–1298, 2015.

[48] Z. Qiu, Y. He, H. Ming, S. Lei, Y. Leng, and Z. Y. Xia, "Lipopolysaccharide (LPS) aggravates high glucose- and hypoxia/reoxygenation-induced injury through activating ROS-dependent NLRP3 inflammasome-mediated pyroptosis in H9C2 cardiomyocytes," *Journal of Diabetes Research*, vol. 2019, Article ID 8151836, 12 pages, 2019.